An application of the coupled-cluster method to the S= 1/2 triangular-lattice antiferromagnet

1995 J. Phys.: Condens. Matter 7 9021

(http://iopscience.iop.org/0953-8984/7/47/020)

J. Phys.: Condens. Matter 7 (1995) 9021–9048. Printed in the UK

An application of the coupled-cluster method to the $S = \frac{1}{2}$ triangular-lattice antiferromagnet

Chen Zeng†, I Staples and R F Bishop

Department of Physics, University of Manchester Institute of Science and Technology (UMIST), PO Box 88, Manchester M60 1QD, UK

Received 23 June 1995

Abstract. The coupled-cluster method is applied to the spin-$\frac{1}{2}$ triangular-lattice anisotropic antiferromagnet, a noncollinear and frustrated magnet with an anisotropy parameter first introduced by Singh and Huse. Various physical quantities including the ground-state energy, the anisotropy susceptibility, the sublattice magnetization, and their critical exponents associated with the magnetic order–disorder quantum phase transition, are calculated by the systematic inclusion of two-spin correlations. These results are then compared and contrasted with those obtained from other methods such as series expansions and variational calculations. The feasibility of carrying out quantum Monte Carlo simulations using the results presented here is also discussed by drawing parallels with the coupled-cluster calculations on the square-lattice antiferromagnets.

1. Introduction

The study of quantum antiferromagnets has undergone a huge resurgence of interest in recent years. Much of this revival has been sparked by the experimental discovery of high-temperature superconductivity in the ceramic cuprate materials [1], and by the theoretical conjecture of Haldane [2] concerning a previously unexpected qualitative difference between the ground-state ordering properties of antiferromagnetic Heisenberg chains with integral and half-odd-integral values of the spin quantum number, S. Nevertheless, despite intense study, many fundamental questions remain unanswered, even for such basic and archetypal systems as the nearest-neighbour Heisenberg model with antiferromagnetic exchange coupling. The only rigorous results [3–6] for the (zero-temperature) ground state of this model Hamiltonian are still all essentially based on the pioneering work of Dyson, Lieb and Simon [3], and from which we now know that Néel order is present to some nonzero degree when $S \geqslant 1$ and when the lattice dimensionality d is such that $d \geqslant 2$.

By contrast, the properties of the physically very interesting $S = \frac{1}{2}$ case are still very much an open question, and the present paper is an attempt to address this problem by bringing to bear upon it a powerful technique from microscopic quantum many-body theory.

Although we shall only be interested in the zero-temperature, $T = 0$, case, we recall that the Mermin–Wagner theorem [7] asserts that any Néel order present at $T = 0$ will be destroyed by thermal fluctuations for $d \leqslant 2$. The only exact results available for the $S = \frac{1}{2}$ case show that the one-dimensional (1D) Heisenberg chain exhibits no Néel order, whereas the three-dimensional (3D) Heisenberg antiferromagnet on a cubic lattice exhibits

† Electronic address: chen@lanczos.ma.umist.ac.uk.

0953-8984/95/479021+28$19.50

nonzero Néel order [6]. To date, no rigorous results are known for the corresponding two-dimensional (2D) $S = \frac{1}{2}$ Heisenberg antiferromagnets. All of the (approximate) results obtained so far indicate that the 2D case is subtle and intriguing. In particular, the lattice geometry seems to play a crucial role, and the presence or absence of frustration appears to be of special importance for determining the ordering present in the ground state. A comparison of the square and triangular lattices is therefore of particular interest in this context.

The technically simpler case of the 2D $S = \frac{1}{2}$ Heisenberg model on the square lattice has been the subject of considerable investigation in recent years [8–30]. The consensus of current opinion from approaches based on spin-wave theory [8, 9, 12], series expansion techniques [10, 16, 18, 22], quantum Monte Carlo (QMC) calculations [11, 13,14, 17,19–21, 24, 25, 27], exact diagonalizations [10, 15, 26], and the coupled-cluster method (CCM) [23, 28–30] is that the $S = \frac{1}{2}$ Heisenberg model on a square lattice exhibits nonzero Néel order at $T = 0$. There is good agreement, for example, that the ground-state staggered (or sublattice) magnetization for the unfrustrated system has a value of about 60–70% of its classical Néel value. It is worth noting that the above consensus concerning the ordering properties of the $S = \frac{1}{2}$ Heisenberg square lattice has depended strongly on the availability of large-scale numerical (QMC) calculations. These have provided very accurate calculations in their own right, and have also proved invaluable as benchmark results against which other *ab initio* microscopic techniques such as the CCM could be compared at various levels of implementation, so that the convergence properties of their approximation schemes could be investigated, for example.

By contrast, the earlier generation of calculations relied heavily on variational approaches. While variational calculations are often an extremely valuable aid in the conceptualization of specific models, they can provide very deceptive results for properties such as order parameters or for correlation functions, even when the corresponding estimates for the energy are good. A typical fairly recent example is a calculation by Liang, Doucot and Anderson [9] for the $S = \frac{1}{2}$ Heisenberg square lattice based on a variational wave function including long-range resonating valence bonds. This trial wave function gives a ground-state energy per spin of -0.6688 ± 0.0004 from a variational Monte Carlo simulation, which is very close to the currently best estimate of $-0.669\,34 \pm 0.000\,04$. Nevertheless, the trial wave function gives a vanishing staggered magnetization, compared to the currently accepted best estimate of about 60–70% of the Néel value. Indeed, Liang *et al* originally argued that that the 2D $S = \frac{1}{2}$ Heisenberg antiferromagnet on the square lattice was close to criticality on the basis that their energy estimate was so accurate. Clearly, such claims are difficult to sustain both in principle and in practice.

By contrast with the case of the $S = \frac{1}{2}$ Heisenberg square-lattice antiferromagnet, the corresponding situation for the frustrated triangular lattice is far less clear. Whereas the square-lattice case has engendered considerable interest in the context of the undoped insulating precursors to the ceramic cuprate materials exhibiting high-temperature superconductivity, the corresponding frustrated triangular (and kagomé) lattices are of interest in the experimental study of such materials as VCl_2 and $NaTiO_2$ [31], and in explaining various anomalous properties of ^3He adsorbed on a graphite substrate [32].

The theoretical study of the triangular Heisenberg antiferromagnet was initiated by Anderson and Fazekas [33, 34]. They suggested that this system might be a prime candidate for a spin liquid, namely a state in which the quantum fluctuations are strong enough to destroy totally the Néel-like order of the classical ground state, which contains three sublattices with spins aligned at 120° to each other. In particular, their proposed resonating-valence-bond (RVB) type of variational wave function implies a disordered spin liquid state.

Other variational calculations have also been performed since then, some of which also exhibit a disordered ground state [35, 36, 37], while others [12, 38] lead to the opposite conclusion of a ground state exhibiting long-range order. For example, Huse and Elser [12] found that their variational estimate for the energy with a wave function of correlated Néel type (i.e., with two- and three-spin correlations on top of a classical three-sublattice state with perfect alignment and relative orientations of 120°) was lower than that with an RVB trial state.

Nevertheless, as we have already discussed in the square-lattice case, conclusions based on variational calculations concerning the presence or absence of long-range order in the real ground state are unreliable, and it is necessary to look to other methods. For example, spin-wave analyses [39–43] lead to the conclusion that quantum fluctuations are insufficient to destabilize the Néel-like long-range order, but imply a sublattice magnetization reduced to about 50% of its classical value. On the other hand, Singh and Huse [44], using a series expansion method, found that the spin-wave results may underestimate the quantum fluctuations. They suggested that the triangular Heisenberg antiferromagnet may be at, or at least very close to, the critical point of Ising magnetic order. Indeed, these authors were the first to introduce an anisotropy parameter into the Hamiltonian, and to calculate such ground-state properties as the energy and sublattice magnetization as functions of this parameter. Their conclusion was that it was difficult to make any definitive statement on the nature of the ground state of the isotropic triangular antiferromagnet using their perturbative approach.

In view of the uncertain nature of the results obtained for the triangular Heisenberg antiferromagnet from the above analytic or semi-analytic approaches, one turns next to large-scale numerical approaches. For the corresponding square-lattice case the results for the largest systems to date have been obtained by various QMC algorithms. These all rely ultimately on a positivity property for the configuration coefficients in the exact wave function. Whereas for the unfrustrated square lattice this condition is guaranteed by the Marshall sign-rule theorem [45], there is no such known result for the frustrated triangular lattice. Thus, the well-known 'sign problem' has so far prevented the application of QMC algorithms to the triangular lattice. Indeed, one of the objectives of the present work is to shed sufficient light on the approximate structure of the nodal surface for the ground-state wave function for QMC algorithms to be able to be applied.

In the absence of any QMC results, essentially all other numerical results for the triangular lattice have come from the exact diagonalization of finite clusters [46–53], followed by an appropriate extrapolation to the thermodynamic limit of an infinite system. To date, clusters of up to 36 spins have been exactly diagonalized. Both the proper quantum-mechanical definition of an order parameter for a finite cluster and the subsequent consistent extrapolation of the finite-size data to the thermodynamic limit are subtle points, as has been stressed by Bernu *et al* [49, 50, 52]. Both steps require a proper understanding of the nature of the symmetry breaking, both for its microscopic quantum features and for the large-scale (i.e., long-wavelength) asymptotic behaviour. Bernu *et al* [52] have argued convincingly that analyses based on incorrect treatments of one or both of these points have led other authors [46–48, 51] performing exact diagonalizations to the incorrect conclusion that the Néel-like magnetic long-range order does not exist in the Heisenberg antiferromagnet.

Bernu *et al* [49] were the first to present numerical evidence of a large set of low-lying levels for the N-spin triangular Heisenberg antiferromagnet, which collapse to the ground state in the $N \to \infty$ thermodynamic limit. These so-called quasi-degenerate joint states are lower in energy than the softest magnons, with the former collapsing to the intensive ground-state energy per spin parameter as N^{-2}, whereas the former collapse as $N^{-\frac{1}{2}}$. It has

been shown [52, 54] that the spontaneous symmetry breaking in quantum antiferromagnets can be described by the collapse of such a set of low-lying quasi-degenerate joint states onto the ground state in the thermodynamic limit, and that they represent precisely the quantum analogue of the classical Néel ground state.

The very recent work of Bernu *et al* [52] presents a careful review of the available exact diagonalization data for the triangular Heisenberg lattice. They argue that its proper interpretation in terms of a consistent description of the symmetries and dynamics of the quasi-degenerate joint states indicates the presence of Néel-like long-range order. Their analysis shows that all of the available data for finite clusters, when properly analysed, are consistent with a value for the staggered magnetization of about 50% of the classical value. This value is essentially identical with the corresponding figure of 48% from lowest-order (i.e., $O(1/S)$) spin-wave theory. Corresponding close agreement between the results of first-order ($O(1/S)$) spin-wave theory [43] and exact diagonalizations of finite lattices [53] has also been found for the spin stiffness, defined in terms of the energy required to impart a small twist to the spins. Since the spin stiffness of a spin liquid is zero and of an ordered antiferromagnet is nonzero, such calculations also provide independent evidence for the existence of Néel-like long-range order, to back that obtained from the presence of a tower of quasi-degenerate joint states in the low-energy spectra of the finite lattices.

Nevertheless, as Bernu *et al* [52] themselves admit, the present state of the art on exact diagonalizations still does not exclude the possibility that for clusters of larger size ($N > 36$) than those studied to date, the quantum fluctuations could drive the system towards criticality, even though there is no evidence of such behaviour in the samples studied ($N \leqslant 36$). In view of the remaining uncertainty it is our intention in the present paper to apply to the triangular-lattice antiferromagnets the fully microscopic coupled-cluster method (CCM) [29, 55–68] which has already been very successfully applied to collinear magnets [23, 28–30], for which it has been shown to be particularly useful in studying the quantum phase transitions [30]. This latter point is particularly pertinent in view of the fact that in such non-collinear antiferromagnets as the triangular lattice the nature of the quantum disorder phase and universal transition are poorly established, despite some attempts in this direction [69].

The CCM has proved to be one of the most powerful and universal *ab initio* techniques in microscopic quantum many-body theory. Among its main advantages are its wide applicability and versatility, its automatic avoidance of unphysical divergences in the thermodynamic limit, and its ability to be implemented at arbitrary accuracy via the existence of systematic hierarchies of approximation schemes. The CCM can be used to calculate ground-state and excited-state energies, and also such other physical quantities as order parameters, correlation functions, and density matrices. It has been applied to a wide range of physical systems, including problems in nuclear physics, both for finite nuclei and infinite nuclear matter; atomic and molecular systems in quantum chemistry; and the electron liquids. More recently, it has also been successfully applied to the problems of quantum anharmonic oscillators treated as $(0+1)$-dimensional field theories; the Φ^4 relativistic quantum field theory; and a model of pions and nuclear interacting via a pseudoscalar coupling. The interested reader is referred to recent reviews [63, 67] for details of these and other calculations.

Over the last few years the CCM has also successfully been applied to many lattice Hamiltonian systems, where it has again been seen to produce results among the best available. [68] and [70] give recent surveys of these results, which include: (i) spin–lattice systems such as the solid phases of ^{3}He [71], and models of interest in magnetism, exemplified by the spin-$\frac{1}{2}$ anisotropic Heisenberg (or *XXZ*-) model [23, 28–30, 71–73], the

spin-1 Heisenberg–biquadratic model [74], and the spin-$\frac{1}{2}$ Majumdar–Ghosh (or J_1–J_2-) model with nearest- and next-nearest-neighbour interactions [75]; (ii) models of strongly interacting electrons on lattices, such as the Hubbard model [76]; and (iii) lattice gauge field theories, such as the Abelian U(1) model [77, 78], and the non-Abelian SU(2) model [79].

The outline of the remainder of this paper is as follows. In section 2 we briefly review the fundamentals of the CCM, and then apply it to the anisotropic spin-$\frac{1}{2}$ triangular-lattice antiferromagnets. The results obtained in the so-called full SUB2 approximation are presented in section 3. We calculate the ground-state energy and sublattice magnetization as functions of the anisotropy parameter, as well as their derivatives. The latter enable us to examine the critical anisotropy and the corresponding critical exponents. We also unearth an interesting oscillatory behaviour concerning the sign of the ket-state correlation coefficients. We conclude in section 4 with a critical discussion of our results.

2. The Hamiltonian, the model state, and the CCM equations

In this section we shall give a very brief review of the coupled-cluster method [55–67] and then apply it to the spin-$\frac{1}{2}$ triangular-lattice antiferromagnets.

2.1. Overview of the coupled-cluster method

The so-called single-reference version of the CCM requires a single model state $|\Phi\rangle$, in terms of which a quantitative and systematic description of the multi-spin correlations can be given. This model state $|\Phi\rangle$ must be a cyclic vector with respect to which one can define two Abelian subalgebras of multi-configurational creation operators $\{C_I^+\}$ and their Hermitian adjoint destruction operators $\{C_I^-\}$. The CCM parametrization of the exact ground-state ket wave function is now written as

$$|\Psi\rangle = \mathrm{e}^S|\Phi\rangle \qquad S = \sum_I s_I C_I^+ \tag{1}$$

where the cluster correlation operator S is decomposed wholly in terms of mutually commuting creation operators $\{C_I^+\}$ for distinct multi-spin excitations with respect to the model state $|\Phi\rangle$. Here $\{s_I\}$ denote the corresponding correlation coefficients which are to be determined. Such an exponential parametrization of the ground state ensures not only the proper counting of the independent multi-spin excitations but also the exact incorporation of the linked-cluster theorem, thereby guaranteeing the size extensivity of any physical quantity under consideration. By taking the inner product of the Schrödinger equation in the form of $\mathrm{e}^{-S}H\mathrm{e}^S|\Phi\rangle = E_g|\Phi\rangle$, with both the reference state itself and the set of multi-spin excitation states, $\{C_I^+|\Phi\rangle\}$, we obtain respectively the ground-state energy:

$$E_g = \langle\Phi|\mathrm{e}^{-S}H\mathrm{e}^S|\Phi\rangle \tag{2}$$

and the coupled set of nonlinear equations:

$$0 = \langle\Phi|C_I^-\mathrm{e}^{-S}H\mathrm{e}^S|\Phi\rangle \tag{3}$$

from which the correlation coefficients $\{s_I\}$ can be determined. It can be seen that this parametrization leads to a workable scheme since the similarity-transformed Hamiltonian, $\mathrm{e}^{-S}H\mathrm{e}^S$, which can be expressed as the nested commutation expansion $H + [H, S] + \frac{1}{2!}[[H, S], S] + \cdots$, actually terminates at a finite order due to the fact that the correlation operator S contains mutually commuting multi-configurational creation operators only, and so long as H is a finite-order multinomial of the elementary single-spin operators, as is the case for almost all models of interest. For example, the similarity-transformed Hamiltonian

will terminate at the fourth order in S if the Hamiltonian H contains products of at most two spin operators.

In order to study arbitrary properties of the system under consideration, the bra state is also needed to calculate expectation values. The overall CCM has two distinct schemes which are known as the normal (NCCM) scheme and the extended (ECCM) scheme, to deal with this [60, 62, 66]. The crux of both schemes is that the corresponding bra and ket states are parametrized independently, and they are therefore no longer manifestly expressed as the Hermitian adjoints of each other. Indeed, this property can be violated when certain levels of approximation are implemented.

The bra ground-state wave function $\langle\tilde{\Psi}|$ corresponding to $|\Psi\rangle$, where $\langle\tilde{\Psi}|H = \langle\tilde{\Psi}|E_g$ is the corresponding Schrödinger equation for the bra state, is parametrized in the NCCM as

$$\langle\tilde{\Psi}| = \langle\Phi|\tilde{S}\mathrm{e}^{-S}. \tag{4}$$

Equations (1) and (4) together with the decomposition

$$\tilde{S} = 1 + \sum_I \tilde{s}_I C_I^- \tag{5}$$

characterize the NCCM. The choice of unity for the constant term in equation (5) implies that $\langle\tilde{\Psi}|\Psi\rangle = \langle\Phi|\Psi\rangle = \langle\Phi|\Phi\rangle = 1$ The ground-state version of the NCCM is now specified completely by the set of parameters $\{s_I, \tilde{s}_I\}$. The expectation value of an arbitrary physical quantity A may be written in the NCCM as

$$\bar{A} = \langle\tilde{\Psi}|A|\Psi\rangle = \langle\Phi|\,\tilde{S}\mathrm{e}^{-S}A\mathrm{e}^{S}\,|\Phi\rangle = \bar{A}\,[s_I, \tilde{s}_I]\,. \tag{6}$$

2.2. The Hamiltonian and the model state

Now that we have given a description of the method that we are using to tackle the problem, we next describe the physical model. The Hamiltonian under consideration describes the $S = \frac{1}{2}$ triangular-lattice Heisenberg antiferromagnet:

$$H = \sum_{(ij)} \left\{ \sigma_i^x \sigma_j^x + \sigma_i^y \sigma_j^y + \sigma_i^z \sigma_j^z \right\} \tag{7}$$

where $\{\sigma_i^x, \sigma_i^y, \sigma_i^z\}$ are the $S = \frac{1}{2}$ Pauli matrices at site i, and the notation (ij) means that the sum is to be over all nearest-neighbour pairs. The triangular-lattice sites are now divided up into three sublattices which we will call the A, B and C sublattices as shown in figure 1(a); the division is done in such a way that no two sites on the same sublattice are nearest neighbours. The classical ground state (i.e., at $S \to \infty$), of the above Hamiltonian is the so-called $\sqrt{3} \times \sqrt{3}$ spin ordering configuration where the spins on the sublattice A point along the negative z-direction, and spins on the sublattices B and C are respectively rotated $+120°$ and $-120°$ away from the negative z-axis in the xz-plane as displayed in figure 1(b).

To facilitate both the extension of the above isotropic Heisenberg antiferromagnet to include an Ising-like anisotropy and the suitable choice of a model state in applying the CCM, we perform a spin-rotation transformation, following Singh and Huse [44], such that the above $\sqrt{3} \times \sqrt{3}$ spin ordering becomes a fully aligned ferromagnetic spin ordering in the spin-rotated coordinates. Specifically, we now rotate about the y-axis the spins on the B and C sublattices by $-120°$ and $120°$ respectively. Therefore, we can rewrite the previous Pauli matrices $\{\sigma_i^x, \sigma_i^y, \sigma_i^z\}$, defined with respect to a global quantization axis, in terms of a new set of Pauli matrices $\{\tilde{\sigma}_i^x, \tilde{\sigma}_i^y, \tilde{\sigma}_i^z\}$ which are now defined with respect to the local

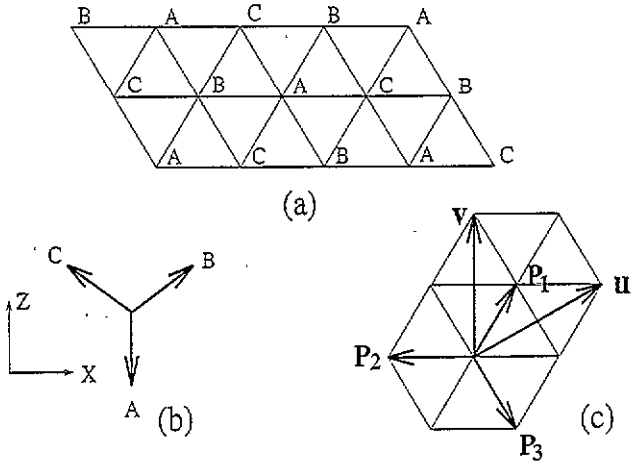

Figure 1. The three-sublattice division of the model state used is indicated by (a). The corresponding spin directions on different sublattices are shown in (b). Some of the vectors introduced in the text are also displayed in (c).

quantization axis at site i due to the spin rotation. For those spins belonging to the B sublattice, for example, we have:

$$\sigma^x = -\frac{1}{2}\tilde{\sigma}^x - \frac{\sqrt{3}}{2}\tilde{\sigma}^z \qquad \sigma^y = \tilde{\sigma}^y \qquad \sigma^z = \frac{\sqrt{3}}{2}\tilde{\sigma}^x - \frac{1}{2}\tilde{\sigma}^z \tag{8}$$

with similar expressions for the spin operators on the C sublattice sites.

Armed with expressions like those given in equation (8), we rewrite the Hamiltonian in terms of spin operators in the spin-rotated coordinates; we also introduce an anisotropy parameter, λ, as below:

$$H(\lambda) = \sum_{\langle i \to j \rangle} \left\{ -\frac{1}{2}\tilde{\sigma}_i^z\tilde{\sigma}_j^z - \frac{\lambda}{2}(\tilde{\sigma}_i^x\tilde{\sigma}_j^x - 2\tilde{\sigma}_i^y\tilde{\sigma}_j^y) + \frac{\sqrt{3}\lambda}{2}(\tilde{\sigma}_i^z\tilde{\sigma}_i^x - \tilde{\sigma}_i^x\tilde{\sigma}_j^z) \right\} \tag{9}$$

so that the Heisenberg Hamiltonian is regained when $\lambda = 1$. The summation is over all nearest neighbours but now with directionality indicated by $\langle i \to j \rangle$ which goes from A to B, B to C, and C to A. *To ease the notational burden, we henceforth drop the tilde symbol on the spin operators.* This should cause no confusion since we will henceforth restrict ourselves entirely to the spin-rotated coordinates. The Hamiltonian can then be rewritten in terms of the corresponding creation and destruction operators, $\sigma^{\pm} = \sigma^x \pm \mathrm{i}\sigma^y$, as

$$H(\lambda) = \sum_{\langle i \to j \rangle} \left\{ -\frac{1}{2}\sigma_i^z\sigma_j^z + \frac{\sqrt{3}\lambda}{4}(\sigma_i^z\sigma_j^+ + \sigma_i^z\sigma_j^- - \sigma_i^+\sigma_j^z - \sigma_i^-\sigma_j^z) \right.$$
$$\left. + \frac{\lambda}{8}(\sigma_i^+\sigma_j^- + \sigma_i^-\sigma_j^+) - \frac{3\lambda}{8}(\sigma_i^+\sigma_j^+ + \sigma_i^-\sigma_j^-) \right\}. \tag{10}$$

Compared with the often-studied *XXZ*-model for extending the isotropic Heisenberg antiferromagnet given in equation (7) to an anisotropic antiferromagnet where the two-spin interaction term $\sigma_i^z\sigma_j^z$ is multiplied by the anisotropy parameter, the present extension represented by (9) or (10) appears somewhat contrived. It facilitates, however, not only the nondegenerate Ising expansion as performed by Singh and Huse [44], but also the implementation of the single-reference version of the CCM outlined above. Unlike the

XXZ-model, whose ground-state manifold has an extensive degeneracy, i.e., a finite entropy per spin, in the limit of vanishing anisotropy, the present anisotropic Hamiltonian given in (9) or (10) at $\lambda = 0$ clearly has as its unique ground state the fully aligned ferromagnetic configuration in the local spin coordinates, whereas the case $\lambda = 1$ recovers the conventional Heisenberg antiferromagnet. We choose this ferromagnetic configuration as our uncorrelated model state in anticipation of a three-sublattice ordering for a wide range of anisotropy starting from $\lambda = 0$. We will denote the model state by $|\Phi\rangle$:

$$|\Phi\rangle = \bigotimes_{i=1}^{N} |\downarrow\rangle_i \qquad \text{in the local quantization axis} \tag{11}$$

where N is the number of lattice sites.

2.3. *The CCM correlation operator and the CCM equations*

To implement the CCM in practice, the correlation operator S has to be truncated. Here we employ the so-called full SUB2 approximation scheme where we retain up to two-spin correlations while higher-order correlations involving more than two spins are set to zero. This truncated S-operator therefore has the following form:

$$S \to S_1 + S_2 = \sum_i A_i \sigma_i^+ + \sum_{ij} B_{ij} \sigma_i^+ \sigma_j^+ \tag{12}$$

where the site indices are allowed to run over all lattice sites. In order to derive the coupled-cluster equations, we must calculate the similarity-transformed Hamiltonian, $\widehat{H} \equiv \mathrm{e}^{-S} H \mathrm{e}^{S}$, which can be readily computed by replacing all the single-spin operators in H with the corresponding similarity-transformed operators, since for any two operators u and v, $\widehat{uv} = \widehat{u}\widehat{v}$. For the SUB2 form of S given in equation (12), we obtain the similarity-transformed single-spin operators as follows:

$$\begin{aligned}
\widehat{\sigma}_i^+ &= \sigma_i^+ \\
\widehat{\sigma}_i^z &= \sigma_i^z + \left[\sigma_i^z, S\right] = \sigma_i^z + 2A_i\sigma_i^+ + 4\sum_l B_{il}\sigma_i^+\sigma_l^+ \\
\widehat{\sigma}_i^- &= \sigma_i^- + \left[\sigma_i^-, S\right] + \frac{1}{2}\left[\left[\sigma_i^-, S\right], S\right] \\
&= \sigma_i^- - 4A_i\sigma_i^z - 8\sum_l B_{il}\sigma_l^+\sigma_i^z - 4(A_i^2 + 2B_{ii})\sigma_i^+ \\
&\quad -16A_i\sum_l B_{il}\sigma_i^+\sigma_l^+ - 16\sum_{lm} B_{il}B_{im}\sigma_i^+\sigma_l^+\sigma_m^+.
\end{aligned} \tag{13}$$

Here the site indices l and m are allowed to run over all lattice sites. Note that the correlation coefficient B_{ii} is only superficially present in the above formulas because of an exact cancellation whenever B_{ii} occurs. The origin of this comes from the basic operator identity $(\sigma_i^+)^2 = 0$ which automatically excludes the unphysical B_{ii} from the correlation operator S. We nonetheless explicitly keep this fictitious term to facilitate the Fourier transform as discussed in appendix A.

To simplify the problem further, we now consider the lattice translational symmetries, in terms of which the set of correlation coefficients $\{A_i\}$ can take one of only three independent values depending on to which sublattice the site index i belongs. For the two-body coefficients, the translational invariance implies that B_{ij} depends only on the difference of its indices, i.e., $B_{ij} = B_{i-j}$. Here $i - j$ is understood as a lattice vector connecting sites i and j, which can be further classified as connecting sites from the A

sublattice to the B sublattice, B to C, C to A, and also A to A, B to B, and C to C. With the prescriptions given by equations (2) and (3), it is a straightforward yet tedious exercise to obtain the ground-state energy expression in terms of these correlation coefficients, and a coupled set of nonlinear equations from which the correlation coefficients can themselves be determined. After deriving these equations by utilizing the translational symmetries only, we also observe that the equations respect an additional symmetry of the cyclic permutation of the three sublattices. The solution to the CCM equations with both the lattice translational and cyclic permutation symmetries being imposed will henceforth be called the symmetric CCM solution. Although the full SUB2 equations may permit other solutions, we restrict ourselves henceforth to the symmetric solution in which the three independent variables from the set $\{A_i\}$ of the single-spin operator S_1 are reduced to just a single variable, denoted by x, and which is now independent of the site index. Similarly, the two-spin correlation coefficients B_{ij}, for a given separation, $i-j$, depend only on whether the spins are on the same or different sublattices regardless of the specification of A, B or C. We thus introduce $\alpha_{i-j} \equiv B_{ij}$ for the former case, and $\varphi_{i-j} \equiv B_{ij}$ for the latter.

From equation (2), we can easily compute the ground-state energy as

$$E_g/N = -1.5 - 18\lambda x^2 - 36\lambda\tilde{\varphi}_0 \tag{14}$$

where $\tilde{\varphi}_0$ denotes the correlation coefficient of a pair of nearest-neighbour spins. Note that we have further introduced $\tilde{\varphi}_{i-j-p_1} \equiv \varphi_{i-j}$ with p_1 being the nearest-neighbour vector as detailed in appendix A.

Similarly we obtain the CCM equation for the single-spin correlation coefficient x as

$$0 = 8x + 4\lambda x + 48\lambda x^3 + 192\lambda x\tilde{\varphi}_0 - 96\lambda x\sum_r(\alpha_r + \tilde{\varphi}_r) \tag{15}$$

where r runs over all lattice vectors of the A sublattice (see appendix A for details). Clearly, a simple inspection of equation (15) shows that $x = 0$ is a solution, the physical origin of which can be traced back to the coplanarity of the spin ordering as discussed in section 3.4 below. We henceforth further restrict ourselves to the coplanar solutions ($x = 0$) of the CCM symmetric equations, although equation (15) may, in principle, also have solutions with $x \neq 0$.

After considerable algebra, we obtain the CCM equations for the two-spin correlation coefficients α_{i-j} and φ_{i-j} by using equation (3), details of which are explicitly given in appendix A. This coupled set of nonlinear equations can be decoupled by performing a Fourier transform (also see appendix A for details). We obtain respectively the equations for the correlation coefficients α_q and $\tilde{\varphi}_q$ in the momentum space as follows (in the case $x = 0$):

$$\begin{aligned} 0 = {} & 24(1 + 24\lambda\tilde{\varphi}_0)\alpha_q + 2\lambda(\tilde{\varphi}_q\Gamma_q + \tilde{\varphi}_q^*\Gamma_q^* - 6\tilde{\varphi}_0) \\ & -48\lambda(\tilde{\varphi}_q\Gamma_q + \tilde{\varphi}_q^*\Gamma_q^*)\alpha_q + 96\lambda\tau_0 - 24\lambda(\tilde{\varphi}_q^2\Delta_q + \tilde{\varphi}_q^{*2}\Delta_q^*) + 48\lambda\eta_0 \end{aligned} \tag{16}$$

and

$$\begin{aligned} 0 = {} & (-4\tilde{\varphi}_0 - 48\lambda\tilde{\varphi}_0^2 - \tfrac{3}{8}\lambda)\Gamma_q^* + (24 + 576\lambda\tilde{\varphi}_0)\tilde{\varphi}_q + 2\lambda(\alpha_q\Gamma_q^* + \tilde{\varphi}_q^*\Delta_q^*) \\ & -24\lambda(\alpha_q^2\Gamma_q^* + \tilde{\varphi}_q^2\Gamma_q + 2\tilde{\varphi}_q\tilde{\varphi}_q^*\Gamma_q^* + 2\alpha_q\tilde{\varphi}_q^*\Delta_q^*) \end{aligned} \tag{17}$$

together with a supplementary constraint

$$0 = \sum_q \alpha_q \tag{18}$$

which ensures that the fictitious variable α_0 ($\equiv B_{ii}$) is zero. Here $\tilde{\varphi}_0$ ($\equiv (3/N)\sum_q \tilde{\varphi}_q$) denotes the correlation coefficient of a pair of nearest-neighbour spins just as in equation

(14). We have also used the shorthand notations $\tau_0 \equiv (3/N)\sum_q \alpha_q \tilde{\varphi}_q \Gamma_q$ and $\eta_0 \equiv (3/N)\sum_q \tilde{\varphi}_q^2 \Delta_q$. Γ_q and Δ_q are defined as $\Gamma_q = 1 + e^{-iq\cdot u} + e^{-iq\cdot v}$ and $\Delta_q = e^{-iq\cdot(u+v)}\Gamma_q^*$ where u and v are the primitive lattice vectors of a sublattice as shown in figure 1(c). Note that in the thermodynamic limit ($N \to \infty$), the vector in the momentum space, q, runs over the first magnetic Brillouin zone, or the first Brillouin zone for one sublattice. We take N to denote the number of spins.

The occurrence of $\tilde{\varphi}_0$, τ_0 and η_0 in the above equations imposes a quantitative self-consistent condition on the solution, which is in contrast to the conventional spin-wave theory or the large-S expansion where the consistency of the assumption of an ordered phase can only be ascertained qualitatively. In order to obtain accurate numerical results for various physical quantities, we discretize the magnetic Brillouin zone and use a large number N_k of points in solving the above CCM equations self-consistently.

Similar procedures have also been carried out for the corresponding CCM bra-state equations where the operator $\tilde{S}$ within the full SUB2 approximation retains the following terms:

$$\tilde{S} \to \tilde{S}_1 + \tilde{S}_2 = 1 + \sum_i c_i \sigma_i^- + \sum_{ij} d_{ij} \sigma_i^- \sigma_j^-. \tag{19}$$

The detailed derivation of the CCM bra-state equations and their Fourier transform are performed in appendix B.

3. Results

In this section, we describe the numerical results for various physical quantities computed within the full SUB2 approximation.

3.1. The ground-state energy

From our calculations we find that the ground-state energy per spin, E_g/N, converges rapidly for increasing N_k. In figure 2 we show E_g/N as a function of the anisotropy parameter λ, where the results obtained by Singh and Huse [44] from a series expansion study are also displayed for comparison. Clearly, the SUB2 results reproduce the corresponding perturbation results very accurately for $\lambda \leqslant 0.5$. At the isotropic Heisenberg point, we obtain $E_g/N = -2.015$, which should be compared with the classical energy of -1.5 and with the value -2.21 ± 0.01 extrapolated from the series expansion [44]. The fact that the SUB2 ground-state energy captures only about 70% of the quantum corrections to the classical energy essentially reflects the significance of three-spin correlations, particularly among three nearest-neighbour spins on an elementary triangle, which are not retained in the SUB2 approximation. To see this more clearly, we tabulate in table 1 the ground-state energy per spin for the isotropic Heisenberg model obtained by other methods. In particular, we note that the variational wave function calculation by Huse and Elser [12] with the inclusion of the nearest-neighbour three-spin correlations yields -2.112 for the ground-state energy per spin, which represents a significant improvement upon the corresponding value of -2.028 obtained by Miyashita with only nearest-neighbour two-spin correlations being considered [38]. Work on the systematic inclusion of higher-order correlations in the CCM on this system is currently in progress.

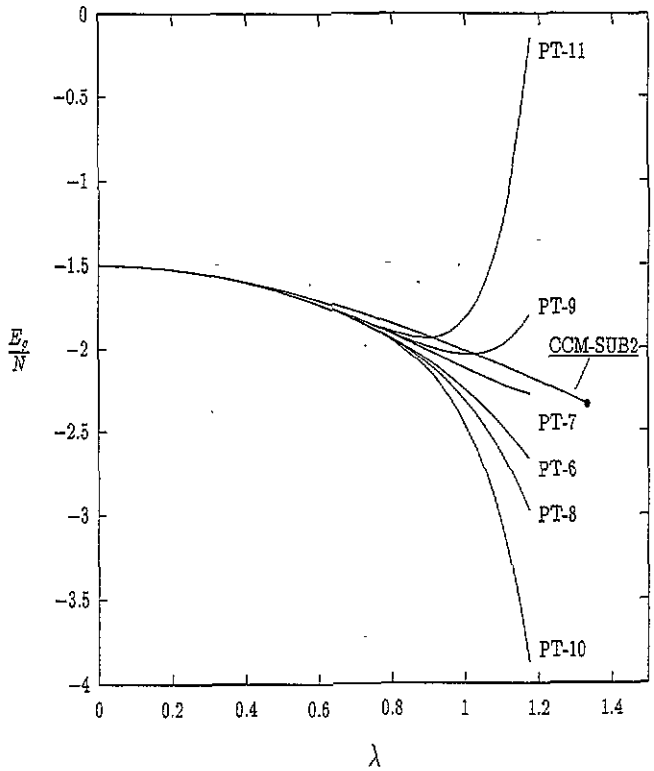

Figure 2. Ground-state energy per spin, E_g/N, as a function of the anisotropy λ. The results from the full SUB2 approximation are obtained with $N_k = 600^2$, where the terminating point is indicated by •, whereas the perturbation results are obtained by Singh and Huse in [44].

Table 1. Comparison of ground-state energies per spin at the Heisenberg point obtained from various methods.

Reference	Method	E_g/N
[38]	Variational[a]	−2.028
[48]	Exact diagonalization	−2.196
[12]	Variational[b]	−2.112
[12]	Variational[c]	−2.1468
[33]	Resonating valence bond	−1.88
[44]	Ising expansion (second order)	−2.174
[44]	Ising expansion (extrapolated)	−2.21
Present work	CCM(SUB2)	−2.015

[a] Only nearest-neighbour two-spin correlations are retained.
[b] Nearest-neighbour two- and three-spin correlations are taken into account.
[c] Two-spin correlations of arbitrary range and the nearest-neighbour three-spin correlations are incorporated.

3.2. The critical anisotropy and the critical exponents

As already hinted in figure 2, the SUB2 ground-state energy curve terminates at an anisotropy λ_c beyond which no physical solution of the CCM equations exists. Although the CCM based on the Néel model state given in equation (11) is bound to break down in the region

of the anisotropy parameter space where the true ground-state wave function possesses a different symmetry from that of the Néel ordering, it is clearly demonstrated in [23] for the square-lattice antiferromagnets that the terminating point corresponds to the critical point of a phase transition. We thus refer to the observed terminating point here for the triangular-lattice anisotropic antiferromagnets as the critical point.

Our method of numerically solving the SUB2 equations is as follows. Since the physical solution to the CCM equations at $\lambda = 0$ requires all the correlation coefficients to be zero, we use this known solution as an initial input in solving the nonlinear CCM equations to obtain the solution for a slightly increased nonzero anisotropy, which, in turn, is used as an initial input for the next incremental anisotropy. We find that $\lambda_c = 1.335\,25 \pm 0.000\,01$. The uncertainty reflects a finite incremented value taken for λ at each step of the iterations.

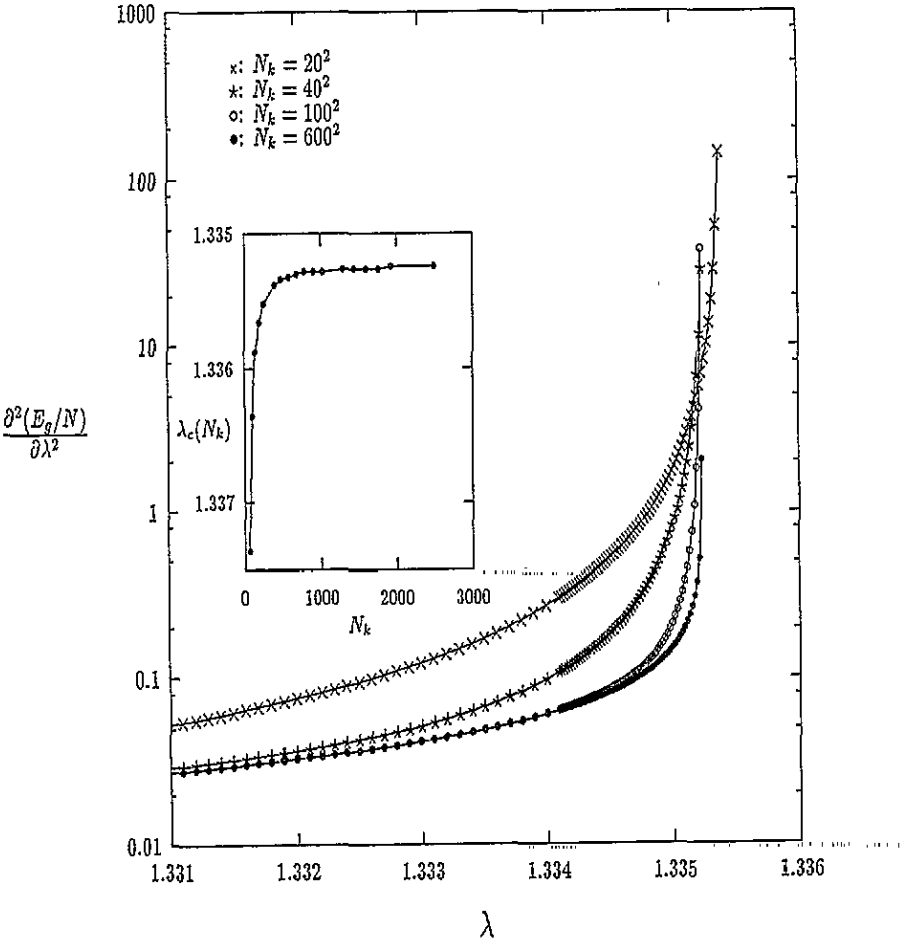

Figure 3. The second derivative of the ground-state energy as a function of the anisotropy. The critical anisotropy as a function of N_k is shown in the inset.

In order to shed further light on the nature of the magnetic order–disorder quantum phase transition in this system by investigating the singular behaviour of the CCM correlation coefficients at the critical point $\lambda = \lambda_c$, we calculate the derivatives of these coefficients with respect to the anisotropy parameter. Since the CCM equations are explicitly given

in equations (15)–(18), we can straightforwardly take the derivatives analytically on both sides of the equations and similarly solve the equations so obtained. By virtue of this, we avoid having to use the numerical difference method for evaluating derivatives and its large associated errors. Recalling that the ground-state energy E_g is related to the nearest-neighbour correlation coefficient φ_0, the above calculation readily yields the derivatives of E_g and reveals the nature of its singularity at λ_c. Specifically, we calculate the anisotropy susceptibility defined as

$$\chi_a \equiv \frac{\partial^2(E_g/N)}{\partial\lambda^2}. \tag{20}$$

The numerical values for χ_a as a function of the anisotropy λ are shown in figure 3 for various numbers of integration points N_k used. Clearly, χ_a diverges at the corresponding critical anisotropy $\lambda_c(N_k)$ which is found to converge quickly with increasing N_k to the value $\lambda_c = 1.335\,25$ quoted above, as can very clearly be seen from the inset in figure 3. In figure 4, we display the log–log plot of the anisotropy susceptibility χ_a versus the deviation of the anisotropy away from the critical value, $\lambda_c - \lambda$. Clearly, in the region where both the deviation is sufficiently small and the convergence has been achieved by increasing N_k, the straight line shows that χ_a has a power-law singularity of the form $\chi_a \sim (\lambda_c - \lambda)^\mu$ as $\lambda \to \lambda_c^-$. The slope readily yields the critical exponent $\mu = -\frac{1}{2}$. Equivalently, the ground-state energy has a $\frac{3}{2}$ power-law singularity at λ_c, or the following expansion near the critical anisotropy:

$$E_g/N \to f_0 + f_1(\lambda_c - \lambda) + f_2(\lambda_c - \lambda)^{\frac{3}{2}} + \cdots \qquad \lambda \to \lambda_c^- \tag{21}$$

where f_0, f_1 and f_2 are constants.

3.3. The sign oscillation of the ket-state correlation coefficients

We now turn our discussion to the structure of the ground-state wave function in connection with the possibility of performing quantum Monte Carlo simulations.

In solving the CCM equations, we have used the fact that all the correlation coefficients are real, and we have correspondingly set $\tilde{\varphi}_{-q} = \tilde{\varphi}_q^*$ in equations (16) and (17). This is justified by noting that the Hamiltonian matrix in a complete basis, for instance, the Ising basis, is real and symmetric. Thus, if a wave function Φ is a ground-state wave function, then Φ^* is also a ground-state wave function; this means that $\Phi + \Phi^* = 2\,\mathrm{Re}\{\Phi\}$ is also a ground-state wave function. From this we deduce that at least one ground-state wave function is real.

Unlike the variational approaches [12, 38], where a certain form such as a power-law decaying behaviour as a function of the separation has to be assumed for the spin–spin correlations to reduce the dimensionality of the parameter space to facilitate the search for the optimal parameters by Monte Carlo simulations, the present SUB2 approximation does not make any *a priori* assumption of this kind. This is important because we can then probe the ground-state structure in an unbiased manner.

For the nonfrustrated antiferromagnets, the essential ingredient is provided by the Marshall–Peierls sign theorem which concerns the phase relations of the projection coefficients of the ground-state wave function onto a complete set of spin configurations [45]. This theorem, when applied to the square Heisenberg antiferromagnet in particular, states that all of the coefficients, when expressed in the spin-rotated coordinates, are positive. Equivalently, the ground-state wave function has only one nodal region, a connected region via the Hamiltonian in the spin configuration space where the wave function has the same

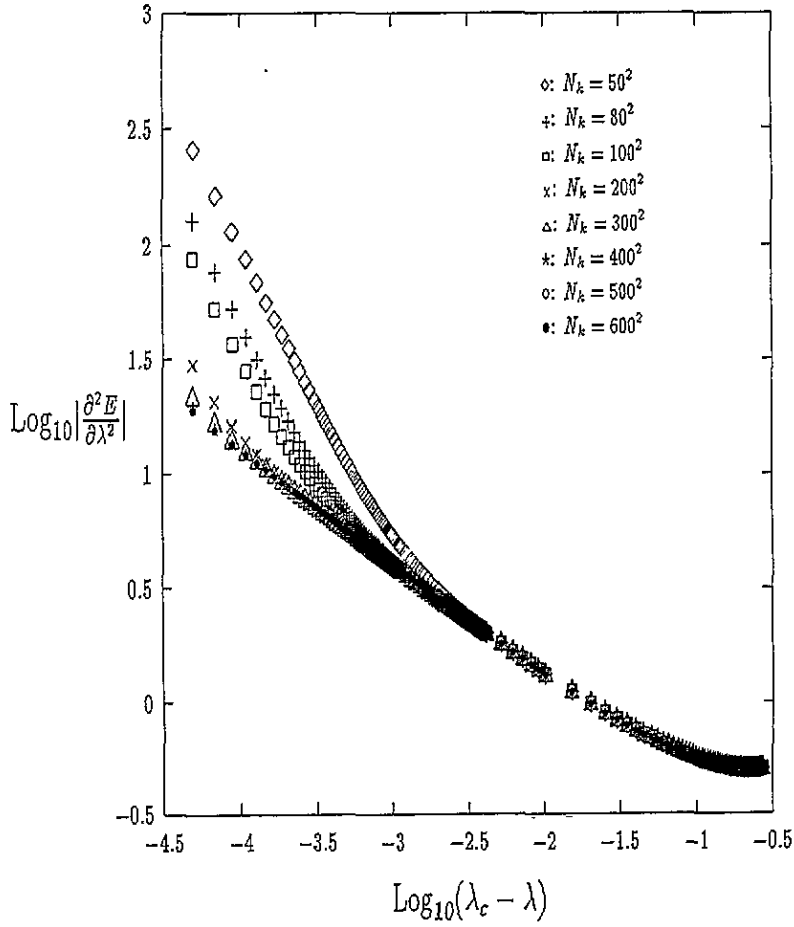

Figure 4. The log–log plot of the anisotropy susceptibility versus the deviation of the anisotropy away from its critical point, for various N_k.

sign. This feature is at the heart of straightforward applications of quantum Monte Carlo simulations [20, 27].

By expanding the exponential operator in the CCM parametrization of the ground ket state, we can easily show that each spin–spin correlation coefficient is a projection coefficient of the ground-state wave function onto the corresponding elementary excitation configuration which flips a pair of spins with respect to the Néel state. Although it is not known *a priori* that the CCM in the SUB2 approximation will satisfy the Marshall sign theorem for the square lattice, the numerical values of these coefficients at the isotropic Heisenberg point plotted in figure 5(a) clearly show that this is the case. By contrast, the corresponding coefficients for the frustrated triangular Heisenberg antiferromagnet are found to have an oscillatory behaviour in their signs, as is also shown in figures 5(a), 5(b) and 5(c). There has been some recent work [80] in which it is argued that the Marshall sign theorem may survive weak frustrations in certain models. However, our present finding is in favour of the breakdown of the Marshall sign theorem for the triangular Heisenberg antiferromagnet. Moreover, more and more correlation coefficients are found to become positive near the terminating point by comparing figure 5(c) with 5(b). This leads us

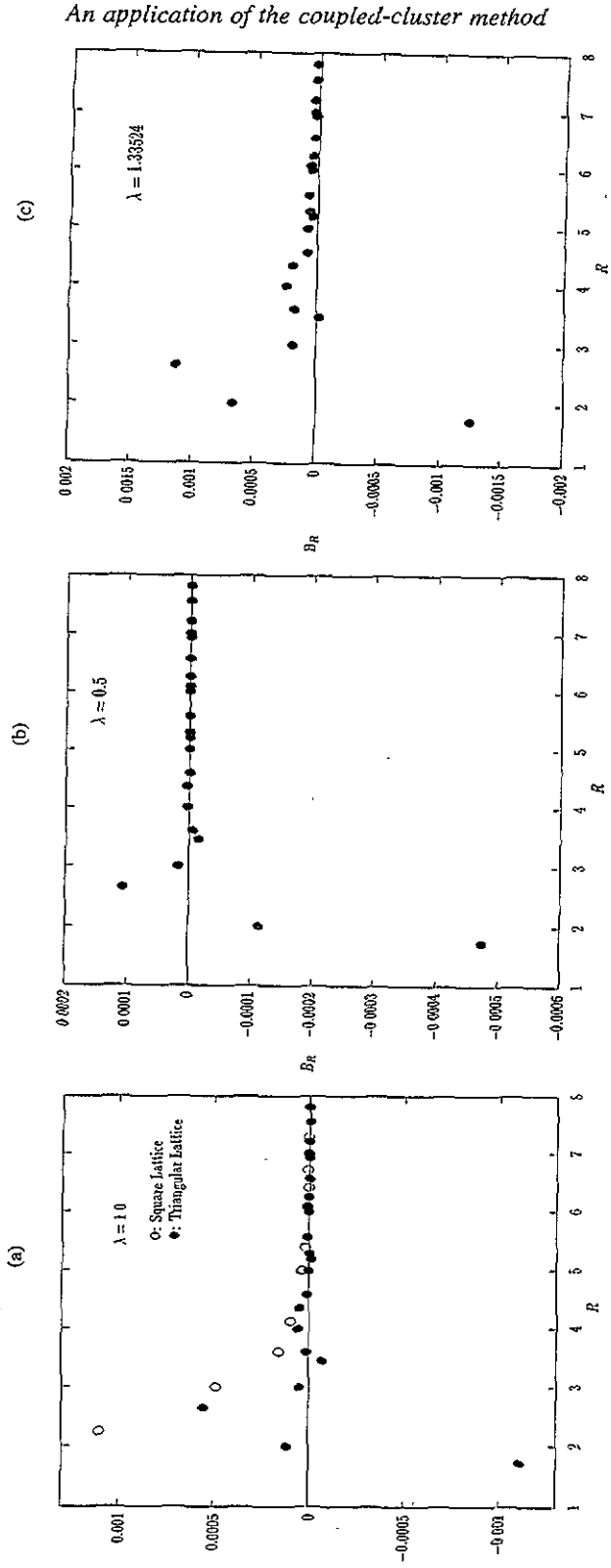

Figure 5. The spin–spin correlation coefficients B_R as a function of the lattice distance R for $\lambda = 1.0$, $\lambda = 0.5$ and $\lambda = 1.335\,24$ are plotted respectively in (a), (b) and (c). At the isotropic Heisenberg point, $\lambda = 1.0$, the corresponding coefficients for the square-lattice antiferromagnet obtained in [23] are also shown in (b) for comparison. Note that we have not displayed the nearest-neighbour correlation coefficient B_1 in order to enlarge the small oscillatory behaviour. All numerical results are obtained with $N_k = 600^2$.

to speculate that the effect due to frustration is considerably suppressed near the critical anisotropy. More interestingly, perhaps, we note that the fixed-node Monte Carlo method [81] and its extension [82] for attacking both continuum and lattice fermion problems require a reliable trial wave function in terms of which the true wave function can be well approximated, especially in terms of its nodal structure. The oscillatory behaviour observed here in the full SUB2 approximation for the frustrated triangular Heisenberg antiferromagnet may represent a reasonable description of the nodal structure of the exact wave function, since we expect corrections from higher-order spin correlations to be small.

3.4. The sublattice magnetization and its critical exponent

We now proceed to use the bra-state correlation coefficients that are obtained from the corresponding bra-state CCM equations, which are given explicitly in appendix B, to compute the sublattice magnetization as a function of the anisotropy parameter λ. The sublattice magnetization M^z is defined to be

$$M^z = -\frac{3}{N}\sum_{n\in A}\langle\sigma_n^z\rangle \tag{22}$$

so we may write directly that

$$M^z = -\frac{3}{N}\sum_{n\in A}\langle\Phi|\tilde{S}e^{-S}\sigma_n^z e^{S}|\Phi\rangle = 1 - \frac{24}{N}\sum_{n\in A}\left(A_n c_n + 24\sum_l B_{nl}d_{nl}\right). \tag{23}$$

Furthermore, we can also compute the out-of-plane component of the sublattice magnetization, $M^y \equiv -(3/N)\sum_{n\in A}\langle\sigma_n^y\rangle$, in terms of which the physical meaning of the single-spin correlation operators S_1 and $\tilde{S}_1$ can be made transparent. To this end, we compute $\langle\sigma_n^y\rangle$ as

$$\langle\sigma_n^y\rangle = \frac{1}{2i}\left(4A_n + 4c_n - 16A_n^2 c_n + 32\sum_l c_l B_{nl} - 512A_n\sum_l B_{nl}d_{nl}\right). \tag{24}$$

Clearly $\langle\sigma_n^y\rangle$ has to be zero; otherwise it gives an unphysical value because of the imaginary factor i. Although the NCCM parametrization, in which the ground ket state $|\Psi\rangle$ and the ground bra state $\langle\tilde{\Psi}|$ are no longer Hermitian conjugates of each other, gives no rigorous guarantee on the reality of any physical quantity calculated within the NCCM scheme, it is shown nonetheless in various contexts that the NCCM does indeed usually give a physical description. Within the well-defined full SUB2 approximation adopted in this paper, we have little choice but to argue for the coplanarity of the spin ordering indicated by $\langle\sigma_n^y\rangle = 0$, which implies that $A_n = c_n = 0$ for arbitrary n. Equivalently, $S_1 = \tilde{S}_1 = 0$.

In figure 6 we show our numerical results for the sublattice magnetization M^z as a function of the anisotropy parameter λ. We find that at the isotropic Heisenberg point ($\lambda = 1$), M^z is about 0.85, or 85% of its classical value. Near the critical point, we show in the inset of figure 6 that the sublattice magnetization at $\lambda = 1.335\,24$ converges rapidly as a function of N_k to about 0.75. To study the singular behaviour of the sublattice magnetization at the critical anisotropy λ_c, we also display in figure 7 the log–log plot of the first derivative of the sublattice magnetization with respect to the anisotropy parameter versus the deviation of the anisotropy away from the critical value, $\lambda_c - \lambda$. In the region where both the deviation is sufficiently small and the convergence has been achieved by increasing N_k, these results reveal a $\frac{1}{2}$ power-law singularity for the sublattice magnetization at λ_c:

$$M^z \to M_c^z + k(\lambda_c - \lambda)^{1/2} + \cdots \qquad \lambda \to \lambda_c^- \tag{25}$$

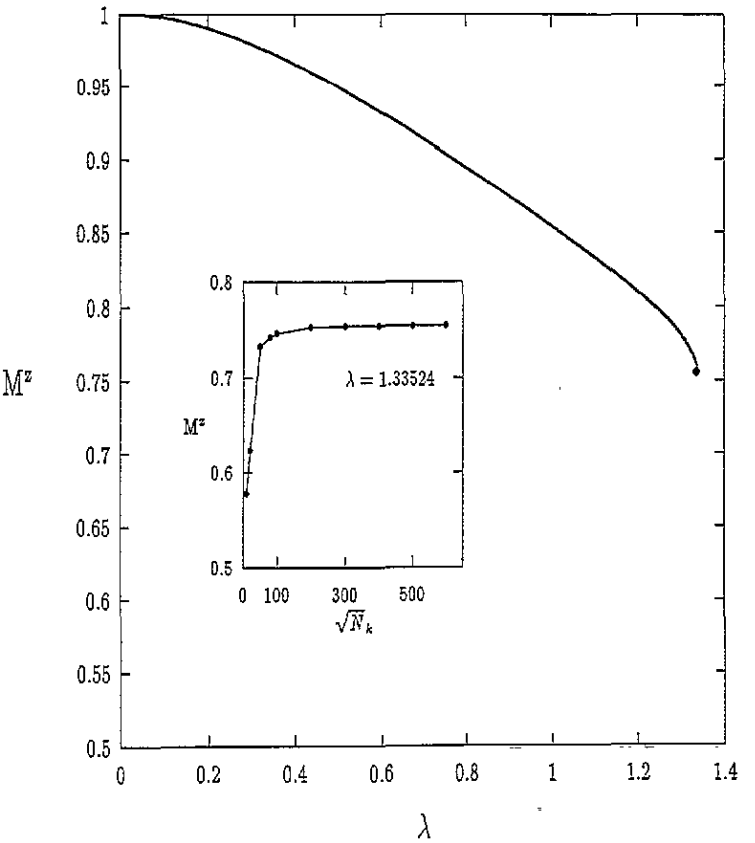

Figure 6. The sublattice magnetization M^z obtained with $N_k = 600^2$ is shown as a function of anisotropy λ. The convergence of M^z against N_k for $\lambda = 1.335\,24$ is displayed as an inset.

where M_c^z and k are constants. Clearly, at the level of the full SUB2 approximation, the ground-state energy and sublattice magnetization have respectively $\frac{3}{2}$ and $\frac{1}{2}$ power-law singularities, which are identical to those for the square-lattice case [30, 83]. This strongly indicates that both phase transitions belong to the same universality class, and further supports the existence of three-sublattice ordering in the frustrated triangular antiferromagnet.

4. Conclusion

In this work, we have extended the domain of application of the CCM to include frustrated antiferromagnets. Arbitrarily long-ranged two-spin correlations are studied and results are derived for the ground-state energy, the anisotropy susceptibility and the sublattice magnetization. This SUB2 calculation is a mean-field type of calculation and has a much wider area of application than merely spin systems. Hence, we recommend its use in the initial study of any system that lends itself to such a method of attack; much in the same way that spin-wave theory is considered now.

The SUB2 calculation presented here has many points of interest in common with spin-wave theory. Both methods use a Gaussian parametrization of the ground-state wave function with an infinite number of parameters. A non-Gaussian parametrization in the

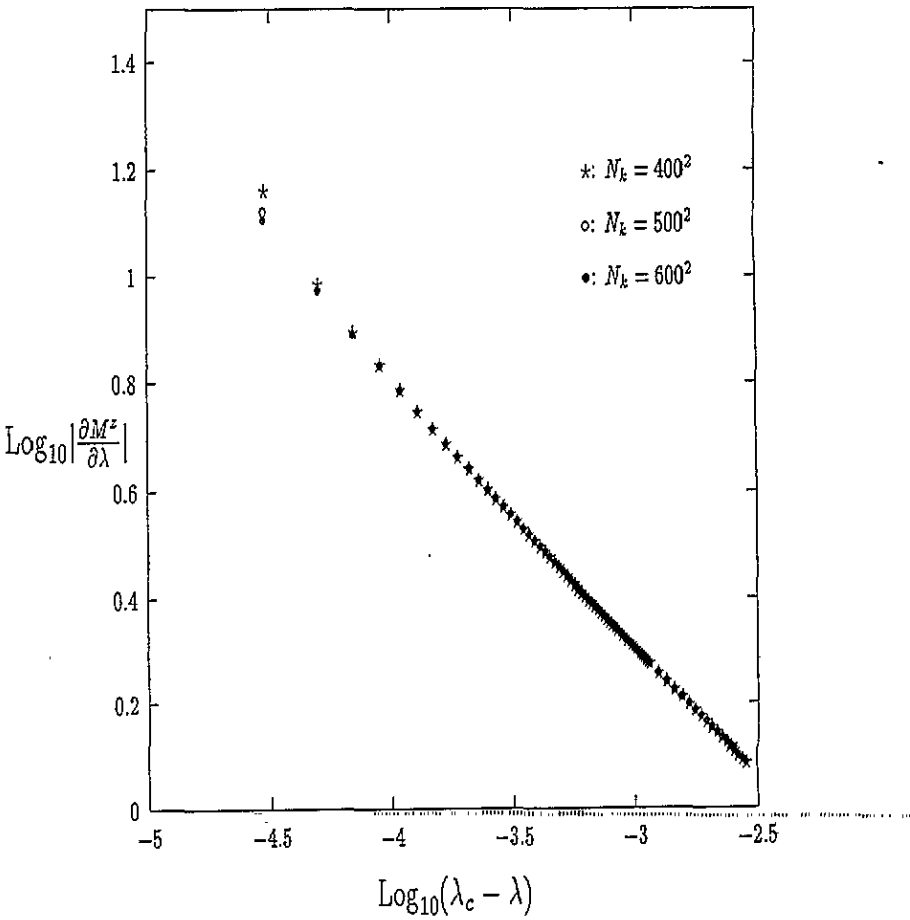

Figure 7. The log–log plot of the first derivative of the sublattice magnetization with respect to the anisotropy versus the deviation of the anisotropy away from its critical point, for various N_k.

CCM with the inclusion of a three-body term on an elementary triangular plaquette is one direction that current work is taking. In contrast to spin-wave theory however, the CCM provides an unbiased estimate of the location of the critical point whereas in spin-wave theory, its existence can be ascertained qualitatively only. To the best of our knowledge, no spin-wave theory analysis has been carried out on this model for a general anisotropy; the only results available being those at $\lambda = 1$ [40].

Much can be gained by comparing the triangular-lattice system under consideration here with the CCM analysis on the square lattice. As has been discussed here and in detail in [84], the triangular lattice and the square lattice are in the same universality class at this level of approximation. In Singh and Huse's paper [44], three scenarios are suggested for the nature of the ground state at the Heisenberg point. The first one is that the ground state has long-range order at $\lambda = 1$; with this assumption the value of the sublattice magnetization is extrapolated to about 20% of its classical value. This value is much smaller than that of the spin-wave calculation, which is about 46% of its classical value [40]. Therefore, they also consider two other possible options: (i) the system disorders at $\lambda = 1$ and (ii) the system disorders at a value $\lambda_c < 1$. For case (i), the system would belong to the universality class

of the classical Heisenberg antiferromagnet on the stacked triangular lattice, whereas for case (ii) it belongs to the universality class of the 3D classical Ising magnet. Both (i) and (ii) will result in a smaller value of the critical exponents for the sublattice magnetization than the value of 1/2 found in the CCM full SUB2 calculations in this paper. Typical values would be around 1/3. Although our mean-field results on the critical exponents support the scenario that the isotropic Heisenberg antiferromagnet possesses a long-ranged three-sublattice ordering, higher-order calculations are needed to carefully identify the universality class of this quantum phase transition.

This also helps to explain why we consider the value of 85% presented here for the sublattice magnetization in this work to be one that can be substantially improved upon by the systematic inclusion of higher-order terms; in this respect, more work needs to be done.

We now turn to the oscillatory nature of the ket-state coefficients, paying particular regard to the implications this could have for the quantum Monte Carlo simulations of such systems at zero temperature. The rule that governs our observed oscillation is not known, although it has been noted that, for increasing values of λ, a greater proportion of coefficients become positive, although no systematic procedure has yet been developed to describe this. Here, the triangular-system ket-state coefficients show a marked difference in behaviour in comparison with the equivalent two-body coefficients for the square lattice. There, the coefficients are all positive in accordance with the Marshall sign rule. This positive semi-definiteness property is what allows quantum Monte Carlo simulations to be carried out on such a system.

In conclusion, the CCM is a fully microscopic method which allows the unbiased and systematic study of quantum phase transitions. On the triangular lattice, higher-order work is required, and it is our hope that the techniques developed in [30] can be adapted to the problem under consideration here and, ultimately, also extended to multi-spin Hamiltonians. This would provide a link with experiment and would present a stern test for the CCM.

Acknowledgments

We acknowledge many useful discussions with J B Parkinson and Y Xian. One of us (CZ) is grateful to C Henley for many valuable suggestions. This work was supported by EPSRC research grant GR-H94986.

Appendix A. The explicit form of the ket-state equations

As indicated in section 2.3, we employ the so-called SUB2 approximation in which all the one- and two-spin correlations are retained while higher-order correlations are set to zero. Thus,

$$S \to S_1 + S_2 = \sum_i A_i \sigma_i^+ + \sum_{ij} B_{ij} \sigma_i^+ \sigma_j^+. \tag{A1}$$

Here, the indices i and j are allowed to run over all lattice sites. In order to derive the coupled-cluster equations, we must now calculate the similarity-transformed Hamiltonian $\mathrm{e}^{-S} H \mathrm{e}^{S}$. As explained in section 2.3, this is done by replacing the single-particle spin operators in the Hamiltonian with their similarity-transformed counterparts.

Now we replace the sum in the Hamiltonian $\sum_{\langle i \to j \rangle}$ over nearest neighbours i, j with a double sum $\sum_i \sum_p$. Here the index i sums over all sites on the lattice, whilst the sum over p denotes a sum over three vectors p_1, p_2, p_3, as shown in figure 1(c), such that if i is on an A sublattice site then $i + p_l, l = 1, 2, 3$, is on a B site. Thus we are replacing j by

$i + p_l$. By this convention, we preserve the condition that $i \rightarrow j$ should always be in the order A→B, B→C and C→A. This condition is due to the directionality of the interaction terms in the Hamiltonian given in equation (10).

In order to derive an equation for the ket-state coefficients A_i and B_{ij}, we apply equation (3). Since we are working in the SUB2 approximation, we have two equations to derive and then solve. The equation for the coefficients A_n is given by

$$0 = \langle \Phi | \sigma_n^- \widehat{H} | \Phi \rangle \tag{A2}$$

and the equation for the coefficients B_{nk} is given by:

$$0 = \langle \Phi | \sigma_n^- \sigma_k^- \widehat{H} | \Phi \rangle . \tag{A3}$$

The equation for the A_n is explicitly obtained as

$$\begin{aligned} 0 = \sum_p \Big\{ & 4A_n + 12A_n^2 \left[A_{n-p} + A_{n+p}\right] + 2\left[B_{n,n+p} - B_{n,n-p}\right] \\ & + \lambda \left[A_{n+p} + A_{n-p}\right] + 4\sqrt{3}\lambda A_n \left[A_{n+p} - A_{n-p}\right] \\ & + 48\lambda A_n \left[B_{n,n+p} + B_{n,n-p}\right] - 24\lambda \sum_i A_i \left[B_{i+p,n} + B_{i-p,n}\right] \Big\} \end{aligned} \tag{A4}$$

whilst the equation for the B_{nk} is

$$\begin{aligned} 0 = \sum_p & \left(8B_{nk}\{1-\delta_{nk}\} - [2A_nA_k + 4B_{nk}]\left\{\delta_{n+p,k} + \delta_{n,k+p}\right\}\right) - \frac{3\lambda}{8}\sum_p \left\{\delta_{n+p,k} + \delta_{n,k+p}\right\} \\ & + \frac{\sqrt{3}\lambda}{2}\sum_p [A_n - A_k]\left\{\delta_{n+p,k} - \delta_{n,k+p}\right\} \\ & + 2\sqrt{3}\lambda \sum_p [A_n - A_k][A_nA_k + 4B_{nk}]\left\{\delta_{n+p,k} - \delta_{n,k+p}\right\} \\ & + 4\sqrt{3}\lambda \sum_p [A_kB_{nn} - A_nB_{kk}]\left\{\delta_{n+p,k} - \delta_{n,k+p}\right\} \\ & + 4\sqrt{3}\lambda \sum_p B_{nk}\left[A_{n+p} + A_{k+p} - A_{n-p} - A_{k-p}\right]\{1-\delta_{nk}\} \\ & + 4\sqrt{3}\lambda \sum_p A_n\left[B_{n+p,k} - B_{n-p,k}\right]\{1-\delta_{nk}\} \\ & + 4\sqrt{3}\lambda \sum_p A_k\left[B_{k+p,n} - B_{k-p,n}\right]\{1-\delta_{nk}\} \\ & - (\lambda/2)\sum_p \left[A_n^2 + A_k^2 + 2B_{nn} + 2B_{kk}\right]\left\{\delta_{n+p,k} + \delta_{n,k+p}\right\} \\ & + \lambda \sum_p \left[B_{n+p,k} + B_{k+p,n}\right]\{1-\delta_{nk}\} + \lambda \sum_p \left[B_{n-p,k} + B_{k-p,n}\right]\{1-\delta_{nk}\} \\ & - 48\lambda \sum_p \left[A_nA_kB_{nk} + B_{nk}^2\right]\left\{\delta_{n+p,k} + \delta_{n,k+p}\right\} \\ & - 6\lambda \sum_p \left[A_n^2 + 2B_{nn}\right]\left[A_k^2 + 2B_{kk}\right]\left\{\delta_{n+p,k} + \delta_{n,k+p}\right\} \\ & + 24\lambda \sum_p B_{nk}\left[A_nA_{n+p} + A_kA_{k+p}\right]\{1-\delta_{nk}\} \end{aligned}$$

$$+24\lambda\sum_p B_{nk}\left[A_{n-p}A_n + A_k A_{k-p}\right]\{1-\delta_{nk}\}$$
$$+12\lambda\sum_p \left[A_n^2 + 2B_{nn}\right]\left[B_{n+p,k} + B_{n-p,k}\right]\{1-\delta_{nk}\}$$
$$+12\lambda\sum_p \left[A_k^2 + 2B_{kk}\right]\left[B_{k+p,n} + B_{k-p,n}\right]\{1-\delta_{nk}\}$$
$$-24\lambda\sum_p\sum_i \left[B_{in}B_{i+p,k} + B_{ik}B_{i+p,n}\right]\{1-\delta_{nk}\}$$
$$+48\lambda\sum_p B_{nk}\left[B_{n,n+p} + B_{k,k+p}\right]\{1-\delta_{nk}\}$$
$$+48\lambda\sum_p B_{nk}\left[B_{n-p,n} + B_{k-p,k}\right]\{1-\delta_{nk}\}. \tag{A5}$$

In equation (A5) above, the term B_{kk} is fictitious and is introduced so that a consistent Fourier transform can be defined. The factor $\{1-\delta_{nk}\}$ which appears repeatedly arises so that the the right-hand side of equation (A5) is identically zero when $n=k$ as implied by equation (A3), since $(\sigma_n^-)^2 = 0$.

We now set about solving these two complicated sets of equations. From the lattice translational symmetry, we assert that $\{A_n\}$ may depend only on what kind of lattice site n lies on; that is, for the $\{A_n\}$ we write

$$A_n = \begin{cases} x & n \in \text{A sublattice} \\ y & n \in \text{B sublattice} \\ z & n \in \text{C sublattice.} \end{cases} \tag{A6}$$

For the $\{B_{nk}\}$, since these correlation coefficients depend only on the difference of their indices, i.e., $B_{nk} = B_{n-k}$, we may write in the case where both indices n and k lie on the same sublattice,

$$B_{nk} = \begin{cases} \alpha_r & n,k \in \text{A sublattice} \\ \beta_r & n,k \in \text{B sublattice} \\ \gamma_r & n,k \in \text{C sublattice} \end{cases} \tag{A7}$$

where in all cases in equation (A7) we have $\boldsymbol{k} = \boldsymbol{n} + \boldsymbol{r}$. Here the bold-type $\boldsymbol{k}$ and $\boldsymbol{n}$ denote the position vectors of the lattice sites k and n respectively. Elements r of set T defined below form a periodic lattice spanned by the sublattice basis $\boldsymbol{u}$ and $\boldsymbol{v}$ as shown in figure 1(c),

$$r \in T = \{w : \boldsymbol{w} = p\boldsymbol{u} + q\boldsymbol{v};\ p,q \in \mathbb{Z}\} \tag{A8}$$

where $\mathbb{Z}$ denotes the set of integers. Thus the lattice is invariant under translation by a vector r when r is a member of the set T defined above. Hence

$$\alpha_r = \alpha_{-r} \qquad \beta_r = \beta_{-r} \qquad \gamma_r = \gamma_{-r}. \tag{A9}$$

For the case when n and k are on dissimilar lattice sites we have

$$B_{nk} = \begin{cases} \varphi_r & n \in \text{A},\ k \in \text{B},\ \boldsymbol{k} = \boldsymbol{n} + \boldsymbol{r} + \boldsymbol{p}_1 \\ \chi_r & n \in \text{B},\ k \in \text{C},\ \boldsymbol{k} = \boldsymbol{n} + \boldsymbol{r} + \boldsymbol{p}_1 \\ \psi_r & n \in \text{A},\ k \in \text{C},\ \boldsymbol{k} = \boldsymbol{n} - \boldsymbol{r} - \boldsymbol{p}_1. \end{cases} \tag{A10}$$

The CCM equations are then rewritten in their entirety using the variables defined above without using any other symmetries other than equation (A9). As the reader will appreciate these equations are very long. However, we find that these equations also respect the

symmetry of cyclic permutation of sublattice A, B, and C. This comes as no surprise since each sublattice is labelled arbitrarily. We therefore restrict ourselves to the SUB2-symmetric solution where

$$\begin{aligned} &x = y = z \\ &\alpha_r = \beta_r = \gamma_r \qquad \forall r \\ &\varphi_r = \chi_r = \psi_r \qquad \forall r. \end{aligned} \tag{A11}$$

With this simplification, equation (A4) for the A_n gives rise to equation (15) used in section 2.3. As discussed there and also in section 3.4, we find that $x = y = z = 0$ is the physical solution, which we call the coplanar solution. With this further restriction ($x = 0$), equation (A5) simplifies considerably, as considered explicitly below.

Thus for the $\{B_{nk}\}$ we have two different cases. Firstly, when n and k are on the same sublattice, we have

$$\begin{aligned} 0 = {} & 24\alpha_r\left[1-\delta_{r,0}\right] + 576\lambda\varphi_{p_1}\alpha_r + 2\sum_p\left[\varphi_{p-r}+\varphi_{p+r}\right] \\ & -24\lambda\sum_p\sum_{r'}\left[\alpha_{r'}\varphi_{r'-r+p}+\varphi_{r'+p_1}\varphi_{r-r'-p-p_1}\right] \\ & -24\lambda\sum_p\sum_{r'}\left[\alpha_{r-r'}\varphi_{r'+p}+\varphi_{-r'-2p_1}\alpha_{r'-r+2p_1+p}\right] \\ & -24\lambda\sum_p\sum_{r'}\left[\varphi_{r'-r+p_1}\varphi_{-r'-p-p_1}+\varphi_{r-r'-2p_1}\alpha_{r'+2p_1+p}\right] \\ & +768\delta_{r,0}\alpha_r\varphi_{p_1} - 2\lambda\delta_{r,0}\sum_p\left[\varphi_{p-r}+\varphi_{p+r}\right] + 48\lambda\delta_{r,0}\sum_p\sum_{r'}\alpha_{r'}\varphi_{r'-r+p} \\ & +48\lambda\delta_{r,0}\sum_p\sum_{r'}\varphi_{r'+p_1}\varphi_{r-r'-p-p_1} \\ & +48\lambda\delta_{r,0}\sum_p\sum_{r'}\varphi_{-r'-2p_1}\alpha_{r'-r+2p_1+p} \end{aligned} \tag{A12}$$

and secondly, when n and k are on different sublattices we have

$$\begin{aligned} 0 = {} & 24\varphi_{r+p_1} + 576\lambda\varphi_{r+p_1}\varphi_{p_1} + 2\lambda\sum_p\left[\alpha_{r+p_1-p}+\varphi_{-r-p-p_1}\right] \\ & -4\left[12\lambda\left(\varphi_{r+p_1}\right)^2+\varphi_{r+p_1}\right]\sum_p\left[\delta_{0,r+p+p_1}+\delta_{r,p-p_1}\right] \\ & -24\lambda\sum_p\sum_{r'}\alpha_{r'}\alpha_{r'-r+p-p_1} - 24\lambda\sum_p\sum_{r'}\varphi_{r'-r+p_1}\varphi_{r'+p} \\ & -24\lambda\sum_p\sum_{r'}\varphi_{r'+p_1}\varphi_{r'-r+p} - 24\lambda\sum_p\sum_{r'}\alpha_{r-r'}\varphi_{-r'-p-p_1} \\ & -24\lambda\sum_p\sum_{r'}\varphi_{r'-2p_1}\varphi_{r-r'-p-p_1} - 24\lambda\sum_p\sum_{r'}\varphi_{r'-r+p_1}\alpha_{r'+2p_1+p}. \end{aligned} \tag{A13}$$

A1. Fourier transformation of the CCM ket-state equations

The further handling of the CCM equations is considerably eased by Fourier transformation. We note that some care must be exercised in performing the Fourier transform, since we require that arguments in the functions describing the spin correlations to be on the same

sublattice as that dummy variable with respect to which the Fourier transformation is made. To remedy this we make use of the following vector relations:

$$3p_1 = u + v \qquad p_2 = -u + p_1 \qquad p_3 = -v + p_1. \tag{A14}$$

We now introduce $\tilde{\varphi}$ so that $\tilde{\varphi}_r \equiv \varphi_{r+p_1}$. This means that φ_{r+p_2} and φ_{r+p_3} are rewritten as $\tilde{\varphi}_{r-u}$ and $\tilde{\varphi}_{r-v}$ respectively. With these changes made, we thus now define the Fourier transform $\tilde{\varphi}_k$ of $\tilde{\varphi}_r$ to be

$$\tilde{\varphi}_k = \sum_{r \in T} \mathrm{e}^{-\mathrm{i}k\cdot r}\tilde{\varphi}_r \tag{A15}$$

with the corresponding inverse being given by

$$\tilde{\varphi}_r = \frac{3}{N}\sum_{k} \mathrm{e}^{\mathrm{i}k\cdot r}\tilde{\varphi}_k \tag{A16}$$

where k runs over the first Brillouin zone of the A sublattice. An equivalent Fourier transform α_k of α_r is also defined.

Before we proceed to Fourier transform the CCM equations for the $\{B_{nk}\}$, and give their solution explicitly, we first note some important points, however. Suppose that there are N_k points in the first Brillouin zone as we discretize it. It can be seen that the number of variables for which we must solve is $3N_k+1$ (namely N_k variables for each α_k, $\tilde{\varphi}_k$, and $\tilde{\varphi}_k^*$, together with $\alpha_{r=0}$), whilst the number of CCM equations we have is $3N_k$. This is because $\alpha_{r=0}$ is a fictitious quantity introduced so that the CCM equations could be self-consistently Fourier transformed. To circumvent this problem, we set $\alpha_{r=0} = 0$ which implies

$$\sum_q \alpha_q = 0 \tag{A17}$$

where the sum over q is over all sites of the first Brillouin zone of the A sublattice. Thus we now have an additional equation, making $3N_k + 1$ equations in all. However, the equations for the α_q are linearly dependent as we shall now show. With the condition $\alpha_{r=0} = 0$ and that of equation (A11), the Fourier-transformed CCM equation for when n and k are on the same sublattice becomes

$$\begin{aligned} 0 = {} & 24\left[1 + 24\lambda\tilde{\varphi}_0\right]\alpha_q + 2\lambda\left[\tilde{\varphi}_q\Gamma_q + \tilde{\varphi}_q^*\Gamma_q^*\right] - 12\lambda\tilde{\varphi}_0 \\ & -48\lambda\alpha_q\left[\tilde{\varphi}_q\Gamma_q + \tilde{\varphi}_q^*\Gamma_q^*\right] + 96\lambda(3/N)\sum_k \alpha_k\tilde{\varphi}_k\Gamma_k \\ & -24\lambda\left[\tilde{\varphi}_q^2\Delta_q + \tilde{\varphi}_q^{*2}\Delta_q^*\right] + 48\lambda(3/N)\sum_k \tilde{\varphi}_k^2\Delta_k \end{aligned} \tag{A18}$$

where we have defined $\Gamma_q = 1 + \mathrm{e}^{-\mathrm{i}q\cdot u} + \mathrm{e}^{-\mathrm{i}q\cdot v}$ and $\Delta_q = \mathrm{e}^{-\mathrm{i}q\cdot(u+v)}\Gamma_q^*$; $\tilde{\varphi}_0 \equiv \varphi_{p_1}$ denotes the nearest-neighbour spin–spin correlation coefficient. Also z^* denotes the complex conjugate of z. This is exactly equation (16) used in section 2.3.

If we now sum equation (A18) over all q then it can be seen that the right-hand side sums identically to zero. Thus our assertion is proved. Therefore, we have only $3N_k$ linearly independent equations. Also note that from equation (A17), the α_q are linearly dependent; that means we only have $3N_k$ linearly independent variables. This discussion arises as we had to introduce the fictitious variable $\alpha_{r=0}$ so that the function α_r is well-defined on an entire sublattice, or the set T in equation (A8), in terms of which a consistent Fourier transform can be defined.

The Fourier transform of equation (A13), when $n \in$ A sublattice and $k \in$ B sublattice, is

$$0 = \left[24 + 576\tilde{\varphi}_0\right]\tilde{\varphi}_q + 2\lambda\left[\alpha_q\Gamma_q^* + \tilde{\varphi}_q^*\Delta_q^*\right] + \left[-4\tilde{\varphi}_0 - 48\lambda\tilde{\varphi}_0^2 - \frac{3}{8}\lambda\right]\Gamma_q^* \\ -24\lambda\left[\alpha_q^2\Gamma_q^* + \tilde{\varphi}_q^2\Gamma_q\right] - 48\lambda\left[\tilde{\varphi}_q\tilde{\varphi}_q^*\Gamma_q^* + \alpha_q\tilde{\varphi}_q^*\Delta_q^*\right]. \tag{A19}$$

This is of course exactly equation (17) quoted in section 2.3.

Throughout the derivation of these Fourier-transformed equations, we have assumed that the ground-state wave function is real. This means that we can write $\tilde{\varphi}_{-q} = \tilde{\varphi}_q^*$. The reality of the ground-state wave function is discussed in section 3.3.

We now bring the reader's attention to an interesting point. We assume that the CCM coefficients in real space are invariant under 120° rotations about the y-axis. Suppose that the rotation of 120° about the y-axis in the positive direction is denoted R_+. Then, the Fourier-transformed quantities we are concerned with in this problem transform as follows:

$$\alpha_{q_+} = \alpha_q \qquad \tilde{\varphi}_{q_+} = \mathrm{e}^{\mathrm{i}q\cdot v}\tilde{\varphi}_q \qquad \Gamma_{q_+} = \mathrm{e}^{-\mathrm{i}q\cdot v}\Gamma_q \qquad \Delta_{q_+} = \mathrm{e}^{-2\mathrm{i}q\cdot v}\Delta_q \tag{A20}$$

where $q_+ = R_+q$. We now consider the CCM equations for the vector q_+ and then make use of the given transformation rules to see if the equations still hold. This was done and no inconsistencies were found. Thus the equation also preserves rotational symmetry.

Although the equations are nonlinear, we now have the same number of variables as equations and so we can try to find a numerical solution of these equations by employing an iterative procedure. This means that great care must be taken in ensuring that the procedure used does not diverge away rapidly when it is in fact close to the correct solution; also, much effort must be devoted to making certain that the iteration map does not enter a domain where there is no solution, thereby halting the algorithm, when in fact if it had chosen a different domain, it would converge to the solution. These points are particularly pertinent when the critical exponents are being calculated when an accuracy to at least five decimal places is required for the value of the critical point and in the ket- and bra-state coefficients. Another point is that, to ensure good accuracy, the largest value of N_k used was $N_k = 600^2$. To decrease the time taken in carrying out the calculation for this value of N_k, data from the iterations involved for $N_k = 500^2$, 400^2 and so on were used in a 'leapfrog' fashion. This reduced the CPU time required dramatically.

Appendix B. The bra-state equations

The ground bra state $\langle\tilde{\psi}|$ is parametrized as

$$\langle\tilde{\psi}| = \langle\Phi|\tilde{S}\mathrm{e}^{-S} \tag{B1}$$

where S is given in equation (12) and $\tilde{S}$ is given by, in the SUB2 approximation,

$$\tilde{S} \to \tilde{S}_1 + \tilde{S}_2 = 1 + \sum_i c_i\sigma_i^- + \sum_{ij} d_{ij}\sigma_i^-\sigma_j^-. \tag{B2}$$

The coefficients c_n and d_{nk} are determined from the equations

$$\langle\Phi|\tilde{S}\mathrm{e}^{-S}\left[H, \sigma_n^+\right]\mathrm{e}^{S}|\Phi\rangle = 0 \tag{B3}$$

and

$$\langle\Phi|\tilde{S}\mathrm{e}^{-S}\left[H, \sigma_n^+\sigma_k^+\right]\mathrm{e}^{S}|\Phi\rangle = 0. \tag{B4}$$

The bra-state equations were derived in the same spirit as equations (A4) and (A5) and are extremely long. They are not given here for reasons of space and we proceed directly to

the methods to verify these equations and the procedure used to solve them. As a check on the consistency of the equations, we may make use of the following observation. Consider the Hamiltonian functional H_{func} where

$$H_{func} = \langle \Phi | \tilde{S} e^{-S} H e^{S} | \Phi \rangle \tag{B5}$$

then

$$\begin{aligned}\frac{\partial H_{func}}{\partial A_n} &= \langle \Phi | \tilde{S} e^{-S} \left[H, \sigma_n^+ \right] e^{S} | \Phi \rangle \\ &= \langle \Phi | e^{-S} \left[H, \sigma_n^+ \right] e^{S} | \Phi \rangle \\ &\quad + \sum_r c_r \langle \Phi | \sigma_r^- e^{-S} \left[H, \sigma_n^+ \right] e^{S} | \Phi \rangle \\ &\quad + \sum_{rs} d_{rs} \langle \Phi | \sigma_r^- \sigma_s^- e^{-S} \left[H, \sigma_n^+ \right] e^{S} | \Phi \rangle \\ &\equiv I_0 + \sum_r c_r I_r^{(1)} + \sum_{rs} d_{rs} I_{rs}^{(2)}. \end{aligned} \tag{B6}$$

However, it can be seen that

$$\begin{aligned} I_0 &= \frac{\partial E}{\partial A_n} \\ I_r^{(1)} &= \frac{\partial}{\partial c_r} \frac{\partial H_{func}}{\partial A_n} = \frac{\partial}{\partial A_n} \left\{ \frac{\partial H_{func}}{\partial c_r} \right\} \\ I_{rs}^{(2)} &= \frac{\partial}{\partial d_{rs}} \frac{\partial H_{func}}{\partial A_n} = \frac{\partial}{\partial A_n} \left\{ \frac{\partial H_{func}}{\partial d_{rs}} \right\}. \end{aligned} \tag{B7}$$

Thus, in order to check the bra-state equations we apply these equations to the expressions that were derived for the ket- and bra-state coefficients. This was done for all the terms in the bra-state equations using expressions like those given in equation (B7). The terms were found to match.

In order to render these equations into a form that enables them to be Fourier transformed, we define new variables μ and τ as follows:

$$d_{nk} = \mu_r \qquad \left\{ \begin{array}{l} n \in \mathrm{A}, k \in \mathrm{A} \\ n \in \mathrm{B}, k \in \mathrm{B} \\ n \in \mathrm{C}, k \in \mathrm{C} \end{array} \right\}, k = n + r \tag{B8}$$

and

$$d_{nk} = \tau_{r+p_1} \qquad \left\{ \begin{array}{l} n \in \mathrm{A}, k \in \mathrm{B} \\ n \in \mathrm{B}, k \in \mathrm{C} \\ n \in \mathrm{C}, k \in \mathrm{A} \end{array} \right\}, k = n + r + p_1. \tag{B9}$$

For the single spin-flip coefficients, we set

$$c_n = c \qquad \forall\, n. \tag{B10}$$

Note that these definitions ensure that the bra-state coefficients satisfy the same symmetric conditions as the ket-state coefficients do in the SUB2-symmetric treatment.

B1. Fourier transformation of the bra-state equations

Now that we have derived the bra-state equations, we must set about solving them. This is done by rewriting the given equations using equations (B8)–(B10) and then Fourier transforming these equations as for the ket-state coefficients. To economize on space, we

proceed directly to the equations once they have been Fourier transformed. For exactly the same reasons that were given in the Fourier transformation of the ket-state coefficients, we define $\tilde{\tau}$ so that $\tilde{\tau}_r \equiv \tau_{r+p_l}$.

We have set $c = 0$; this again reflects the coplanar nature of the system. Also, the set of Fourier-transformed bra-state equations for when $n, k \in$ A sublattice has the same linear dependence property as in the ket-state equations. Therefore, for the same reasons as given earlier, we may set $\mu_{r=0} = 0$. Hence, the Fourier-transformed equation for when $n, k \in$ A sublattice is

$$\begin{aligned}0 = {} & 24\mu_q + 2\lambda\left[\tilde{\tau}_q\Gamma_q + \tilde{\tau}_q^*\Gamma_q^* - 6\tilde{\tau}_0\right] + 576\lambda\tilde{\varphi}_0\mu_q - 48\lambda\left[\mu_q\tilde{\varphi}_q\Gamma_q + \tilde{\tau}_q\tilde{\varphi}_q\Delta_q\right] \\ & -48\lambda\left[\alpha_q\tilde{\tau}_q\Gamma_q + \mu_q\tilde{\varphi}_q^*\Gamma_q^*\right] - 48\lambda\left[\tilde{\tau}_q^*\tilde{\varphi}_q^*\Delta_q^* + \alpha_q\tilde{\tau}_q^*\Gamma_q^*\right] \\ & +48\lambda(3/N)\sum_k\left[\tilde{\tau}_k\tilde{\varphi}_k\Delta_k + \mu_k\tilde{\varphi}_k\Gamma_k\right] + 48\lambda(3/N)\sum_k\left[\alpha_k\tilde{\tau}_k\Gamma_k + \alpha_k\tilde{\tau}_k^*\Gamma_k^*\right] \\ & +48\lambda(3/N)\sum_k\left[\mu_k\tilde{\varphi}_k^*\Gamma_k^* + \tilde{\tau}_k^*\tilde{\varphi}_k^*\Delta_k^*\right] \qquad \text{(B11)}\end{aligned}$$

and for when $n \in$ A, $k \in$ B the Fourier-transformed equation is

$$\begin{aligned}0 = {} & 24\tilde{\tau}_q - \frac{3}{8}\lambda\Gamma_q^* - 4\tilde{\tau}_0\Gamma_q^* + 2\lambda\left[\mu_q\Gamma_q^* + \tilde{\tau}_q^*\Delta_q^*\right] + 576\lambda\tilde{\varphi}_0\tilde{\tau}_q - 96\lambda\tilde{\varphi}_0\tilde{\tau}_0\Gamma_q^* \\ & +96\lambda(3/N)\sum_k\left[\alpha_k\mu_k + 2\tilde{\varphi}_k\tilde{\tau}_k^*\right]\Gamma_q^* - 48\lambda\left[\alpha_q\tilde{\tau}_q^*\Delta_q^* + \tilde{\varphi}_q\tilde{\tau}_q^*\Gamma_q^*\right] \\ & -48\lambda\left[\tilde{\tau}_q\tilde{\varphi}_q\Gamma_q + \mu_q\tilde{\varphi}_q^*\Delta_q^*\right] - 48\lambda\left[\tilde{\tau}_q\tilde{\varphi}_q^*\Gamma_q^* + \alpha_q\mu_q\Gamma_q^*\right] \qquad \text{(B12)}\end{aligned}$$

together with the supplementary constraint

$$0 = \sum_q \mu_q. \qquad \text{(B13)}$$

Note that the equations (B11) and (B12) are linear in the unknown variables $\{\mu_q\}$ and $\{\tilde{\tau}_q\}$, which means that these equations are much easier to solve numerically provided that the ket-state coefficients $\{\alpha_q\}$ and $\{\tilde{\varphi}_q\}$ are known.

References

[1] Bednorz J G and Müller K A 1986 Z. *Phys.* B **64** 189
[2] Haldane F D M 1983 *Phys. Lett.* **93A** 464; 1983 *Phys. Rev. Lett.* **50** 1153
[3] Dyson F J, Lieb E H and Simon B 1978 *J. Stat. Phys.* **18** 335
[4] Jordao Neves E and Fernando Perez J 1986 *Phys. Lett.* **114A** 331
[5] Affleck I, Kennedy T, Lieb E H and Tasaki H 1988 *Commun. Math. Phys.* **115** 477
[6] Kennedy T, Lieb E H and Shastry B S 1988 *J. Stat. Phys.* **53** 1019
[7] Mermin N D and Wagner H 1966 *Phys. Rev. Lett.* **17** 1133
[8] Anderson P W 1952 *Phys. Rev.* B **86** 694
Oguchi T 1960 *Phys. Rev.* B **117** 117
[9] Liang S, Doucot B and Anderson P W 1988 *Phys. Rev. Lett.* **61** 365
[10] Huse D 1988 *Phys. Rev.* B **37** 2380
[11] Reger J D and Young A P 1988 *Phys. Rev.* B **37** 5978
[12] Huse D A and Elser V 1988 *Phys. Rev. Lett.* **60** 2531
[13] Gross M, Sanchez-Velasco E and Siggia E 1989 *Phys. Rev.* B **39** 2484
[14] Barnes T, Kotchan D and Swanson E S 1989 *Phys. Rev.* B **39** 4357
[15] Tang S and Hirsch J E 1989 *Phys. Rev.* B **39** 4548
[16] Singh R R P 1989 *Phys. Rev.* B **39** 9760
[17] Carlson J 1989 *Phys. Rev.* B **40** 846
[18] Singh R R P and Huse D A 1989 *Phys. Rev.* B **40** 7247
[19] Liu Z and Manousakis E 1989 *Phys. Rev.* B **40** 11437

[20] Trivedi N and Ceperley D M 1990 *Phys. Rev.* B **41** 4552
[21] Liang S 1990 *Phys. Rev.* B **42** 6555
[22] Zheng W, Oitmaa J and Hamer C J 1991 *Phys. Rev.* B **43** 8321
[23] Bishop R F, Parkinson J B and Xian Y 1991 *Phys. Rev.* B **43** 13782; *Phys. Rev.* B 1991 **44** 9425
[24] Barnes T 1991 *Int. J. Mod. Phys.* B **2** 659
[25] Manousakis E 1991 *Rev. Mod. Phys.* **63** 1
[26] Schultz H and Ziman T 1992 *Europhys. Lett.* **8** 355
[27] Runge K J 1992 *Phys. Rev.* B **45** 12292
[28] Harris F E 1993 *Phys. Rev.* B **47** 7903
[29] Bishop R F and Xian Y 1994 *Int. J. Quantum Chem.: Quantum Chem. Symp.* **28** 155
[30] Bishop R F, Hale R G and Xian Y 1994 *Phys. Rev. Lett.* **73** 3157
[31] Harrison A 1992 *Annu. Rep. Prog. Chem.* **87A** 211
[32] Greywall D S and Busch P A 1989 *Phys. Rev. Lett.* **62** 1868
Siqueira M, Cowan C P and Saunders J 1993 *Phys. Rev. Lett.* **71** 1407
Schiffer P, O'Keefe M T and Osheroff D D 1993 *Phys. Rev. Lett.* **71** 1403
[33] Anderson P W 1973 *Mater. Res. Bull.* **8** 153
[34] Fazekas P and Anderson P W 1974 *Phil. Mag.* **30** 432
[35] Oguchi T, Nishimori H and Taguchi Y 1986 *J. Phys. Soc. Japan* **55** 323
[36] Kalmeyer V and Laughlin R B 1987 *Phys. Rev. Lett* **59** 2095
[37] Yang K, Warman L K and Girvin S M 1993 *Phys. Rev. Lett.* **70** 2641
[38] Miyashita S 1984 *J. Phys. Soc. Japan* **53** 44
[39] Nishimori H and Miyake S J 1985 *Prog. Theor. Phys.* **73** 18
[40] Jolicoeur T and LeGuillou J C 1989 *Phys. Rev.* B **40** 2727
[41] Miyake S J 1992 *J. Phys. Soc. Japan* **61** 983
[42] Aoki T 1993 *J. Phys. Soc. Japan* **62** 2462
[43] Chubukov A V, Sachdev S and Senthil T 1994 *J. Phys.: Condens. Matter* **6** 8891
[44] Singh R R P and Huse D A 1992 *Phys. Rev. Lett.* **68** 1766
[45] Marshall W 1955 *Proc. R. Soc.* A **232** 48
[46] Fujiki S 1987 *Can. J. Phys.* **65** 489
[47] Imada M 1987 *J. Phys. Soc. Japan* **56** 311; 1989 *J. Phys. Soc. Japan* **58** 2650
[48] Nishimori H and Nakanishi H 1988 *J. Phys. Soc. Japan* **57** 626
[49] Bernu B, Lhuillier C and Pierre L 1992 *Phys. Rev. Lett.* **69** 2590
[50] Bernu B, Lecheminant P, Lhuillier C and Pierre L 1993 *Phys. Scr.* T **49** 192
[51] Leung P W and Runge K J 1993 *Phys. Rev.* B **47** 5861
[52] Bernu B, Lecheminant P, Lhuillier C and Pierre L 1994 *Phys. Rev.* B **50** 10048
[53] Lecheminant P, Bernu B, Lhuillier C and Pierre L 1994 *Preprint*
[54] Azaria P, Delamotte B and Mouhanna D 1993 *Phys. Rev. Lett.* **70** 2483
[55] Coester F 1958 *Nucl. Phys.* **7** 421
Coester F and Kümmel H 1960 *Nucl. Phys.* **17** 477
[56] Čížek J 1966 *J. Chem. Phys.* **45** 4256; 1969 *Adv. Chem. Phys.* **14** 35
[57] Paldus J, Čížek J and Shavitt I 1972 *Phys. Rev.* A **5** 50
[58] Bishop R F and Lührmann K H 1978 *Phys. Rev.* B **17** 3757; 1982 *Phys. Rev.* B **26** 5523
[59] Kümmel H, Lührmann K H and Zabolitzky J G 1978 *Phys. Rep.* C **36** 1
[60] Arponen J 1983 *Ann. Phys., NY* **151** 311
[61] Bishop R F and Kümmel H G 1987 *Phys. Today* **40** (3) 52
[62] Arponen J S, Bishop R F and Pajanne E 1987 *Phys. Rev.* A **36** 2519; 1987 *Phys. Rev.* A **36** 2539; 1987 *Condensed Matter Theories* vol 2, ed P Vashishta, R K Kalia and R F Bishop (New York: Plenum) p 357
[63] Bartlett R J 1989 *J. Phys. Chem.* **93** 1697
[64] Arponen J S and Bishop R F 1990 *Phys. Rev. Lett.* **64** 111
[65] Bishop R F and Arponen J S 1990 *Int. J. Quantum Chem.: Quantum Chem. Symp.* **24** 197
[66] Arponen J S and Bishop R F 1991 *Ann. Phys., NY* **207** 171; 1993 *Ann. Phys., NY* **227** 275, 334
[67] Bishop R F 1991 *Theor. Chim. Acta* **80** 95
[68] Bishop R F and Xian Y 1994 *Condensed Matter Theories* vol 9, ed J W Clark, K A Shoaib and A Sadiq (Commack, NY: Nova Science) p 433
[69] Read N and Sachdev S 1989 *Phys. Rev. Lett.* **62** 1694
[70] Bishop R F 1995 *Recent Progress in Many-Body Theories* vol 4, ed E Schachinger, H Mitter and H Sormann (New York: Plenum) p 195
[71] Roger M and Hetherington J H 1990 *Phys. Rev.* B **41** 200

[72] Bishop R F, Parkinson J B and Xian Y 1992 *J. Phys.: Condens. Matter* **4** 5783
[73] Cornu F, Joliceur T and LeGuillou J C 1994 *Phys. Rev.* B **49** 9548
[74] Bishop R F, Parkinson J B and Xian Y 1993 *J. Phys.: Condens. Matter* **5** 9169
[75] Farnell D J J and Parkinson J B 1994 *J. Phys.: Condens. Matter* **6** 5521
Xian Y 1994 *J. Phys.: Condens. Matter* **6** 5965
[76] Roger M and Hetherington J H 1990 *Europhys. Lett.* **11** 255
Lo C F, Manousakis E and Wang Y L 1991 *Phys. Lett.* **156A** 42
Petit F and Roger M 1994 *Phys. Rev.* B **49** 3453
Bishop R F, Xian Y and Zeng C 1995 *Int. J. Quantum Chem.* **55** 181
[77] Bishop R F, Kendall A S, Wong L Y and Xian Y 1993 *Phys. Rev.* D **48** 887; 1993 *Condensed Matter Theories* vol 8, ed L Blum and F B Malik (New York: Plenum) p 269
[78] Bishop R F and Xian Y 1993 *Acta Phys. Pol.* **24** 541; 1994 *Nucl. Phys. (Proc. Suppl.)* B **34** 808
[79] Llewellyn Smith C H and Watson N J 1993 *Phys. Lett.* **302B** 463
[80] Richter J, Ivanov N B and Retzlaff K 1994 *Europhys. Lett* **25** 545
Zeng C and Parkinson J B 1995 *Phys. Rev.* B **51** 11 609
[81] Ceperley D M and Alder B J 1980 *Phys. Rev. Lett.* **45** 566; 1986 *Science* **231** 555
[82] van Bemmel H J M, ten Haaf D F B, van Saarloos W, van Leeuwen J M J and An G 1994 *Phys. Rev. Lett.* **72** 2442
[83] Zeng C, Staples I and Bishop R F 1995 *UMIST Preprint*